PII: S0032-3861(96)00748-3

Polymer Vol. 38 No. 9, pp. 2251–2257 1997

0032-3861/97/$17.00 + 0.00

Structure and molecular motion of polystyrene chains adsorbed on porous silica surfaces by the spin label method

Shigetaka Shimada* and Akinori Sugimoto
Nagoya Institute of Technology, Gokiso-cho, Showa-ku, Nagoya 466, Japan

and Masami Kawaguchi
Mie University, 1515 Kamihama-cho, Tsu Mie 514, Japan
(Received 15 May 1996; revised 4 July 1996)

The spin-label method has been used to study the structure and molecular motion of polystyrene chains adsorbed on porous silica. Spin-labelled polystyrene (PS) with a narrow molecular weight distribution, having M_w (weight average molecular weight) $= 1.9 \times 10^5$ was adsorbed on the surface of porous silica with two different pore diameters, 28.5 nm (MB-300) and 81.3 nm (MB-800), in cyclohexane (C_6H_{12}) and carbon tetrachloride (CCl_4) solutions at 35°C. E.s.r. spectra were observed at various temperatures after the samples were completely dried. The anisotropic hyperfine splitting due to nitrogen nucleus observed at −196°C, which is a good measure of the magnitude of the PS–silica interaction, is larger for the adsorbed PS from the CCl_4 solution and the PS on the silica with the larger pore diameter. The molecular mobility of the PS chains was estimated from temperature dependence of the e.s.r. spectra. It is found that the conformations of the PS chains in the Θ (C_6H_{12}) and good (CCl_4) solvents affect the structures of adsorbed PS on the silica surface and the molecular mobility decreases with increasing PS–silica interaction. © 1997 Elsevier Science Ltd.

(Keywords: polystyrene; silica surface; adsorption)

INTRODUCTION

Polymer adsorption phenomena have been studied intensively to understand the structure and molecular dynamics of polymer chains near solid surfaces[1–5]. Many investigations by e.s.r. and i.r. methods[6–9] have been published concerning adsorption of polymer. Recently, Kawaguchi *et al.*[10–12] studied the adsorption behaviour of polystyrene on different porous silica in order to examine the effect of surface geometry on the adsorption. They concluded that the adsorption isotherm is a function of the size ratio of the average pore diameter to the radius gyration of a PS chain. The effect of the surface geometry on the PS adsorption motivated us to characterize the segment–surface interaction and the molecular motion of the segment. The structure of the weakly interacting polymer–solid surface and the nature of the polymer–solid interface characterized by strong and specific interactions should be clarified by the spin-label study of the PS adsorbed on the porous silica surfaces with different pore diameters. For simplicity, we study the adsorption of a polystyrene with a narrow molecular distribution, having $\overline{M_w} = 1.9 \times 10^5$, on well-defined porous silicas in cyclohexane and in carbon tetrachloride. The difference of the solvent power affects the radius of gyration of the PS in the solutions. In this paper we provide a simple model of the structures of the adsorbed PS from the solutions related to molecular motion.

* To whom correspondence should be addressed

EXPERIMENTAL

Materials

A polystyrene having $\overline{M_w}$ (weight average molecular weight) $= 1.9 \times 10^5$ (PS-190) was purchased from Tosoh Co. (Tokyo, Japan). The polydispersity of the PS-190 was 1.04. The polystyrene was spin-labelled by the method of Bullock *et al.*[13]. The labelled monomer unit has the structure

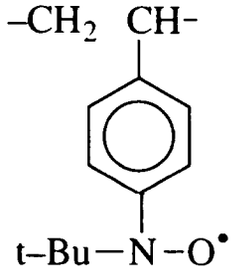

The labelled polymers (SL–PS) were finally purified by precipitating three times from toluene solution by addition of methanol and dried under vacuum for more than 1 day at room temperature. The porous silica particles used for the adsorbent were micro bead (100–200 mesh) silica gels, MB-300 and MB-800 of Fuji-David Chemical Co., Kasugai, Japan. The surface

area, the pore size and the method of characterization were mentioned in ref. 10. The average pore diameters (d) of the silica gels, MB-300 and MB-800, are 28.5 nm and 81.3 nm, respectively. The silica particles were purified by washing by hot carbon tetrachloride and dried in a vacuum oven at 130–150°C for several days.

Adsorption of polystyrene

A small amount of SL–PS (0.03 g) was dissolved in 2 ml of cyclohexane (C_6H_{12}) or carbon tetrachloride (CCl_4). A fixed amount of silica was transferred to an e.s.r. sample tube to maintain a similar total surface area for the different silica particles (0.0115 g for MB-300 and 0.0302 g for MB-800) and then the PS solution was mixed with the silica particles. The sample in the tube was placed and shaken in an ultrasonic cleaner for 10 min at 35°C in order to allow the solution to fully penetrate into the pores. After the silica particles were sedimented, the supernatant was carefully removed by an injector. In order to confirm adsorption of polystyrene, e.s.r. spectra of the residue were observed and compared with the spin-labelled PS in solutions of C_6H_{12} and CCl_4. After the e.s.r. measurements, the residue in the sample tube was dried in the vacuum oven at 40°C for several days. The same procedures for different silica samples were performed. After the solvents were completely evacuated, e.s.r. measurements were carried out in order to study structure and molecular motion of PS adsorbed on the dried silica. The four samples obtained were coded as MB-300/C_6H_{12}, MB-800/C_6H_{12}, MB-300/CCl_4 and MB-800/CCl_4.

E.s.r. measurements

E.s.r. measurements were carried out with a JEOL FE3XG and a JEOL ME3XG spectrometer and a connected PC9801 computer. The signal of diphenylpicrylhydrazyl (DPPH) was used as a g-value standard. The magnetic field sweep was calibrated with the known splitting constant of Mn^{2+} in MnO.

Simulation

Computer simulation was carried out in order to obtain the principal values of **g** and **A** tensors and the line width. Since it was reasonable to assume that the nitroxide radicals have a completely random orientation, the **g** and **A** values could be computed from equations (1) and (2),

$$\mathbf{g} = (g_x^2 \sin^2\theta \sin^2\phi + g_y^2 \sin^2\theta \cos^2\phi + g_z^2 \cos^2\theta)^{1/2} \quad (1)$$

$$\mathbf{A} = (g_x^2 A_x^2 \sin^2\theta \sin^2\phi + g_y^2 A_y^2 \sin^2\theta \cos^2\phi + g_z^2 A_z^2 \cos^2\theta)^{1/2} \quad (2)$$

choosing the 8100 sets of (θ, ϕ) in a solid angle of $\pi/2$, where g_x, g_y and g_z, are the principal values of the **g** tensor and A_x, A_y, and A_z are those of the **A** tensor due to the nitrogen nucleus. It was also assumed that the principal directions of the **g** and **A** tensors coincided. θ and ϕ are polar and azimuthal angles, respectively, in the principal axis system (x, y, z). Several theoretical spectra were calculated by gradually changing the principal values and the line width of the Gaussian line shape function. These spectra were recorded on an x–y plotter and compared with the observed spectra in order to get the best fit.

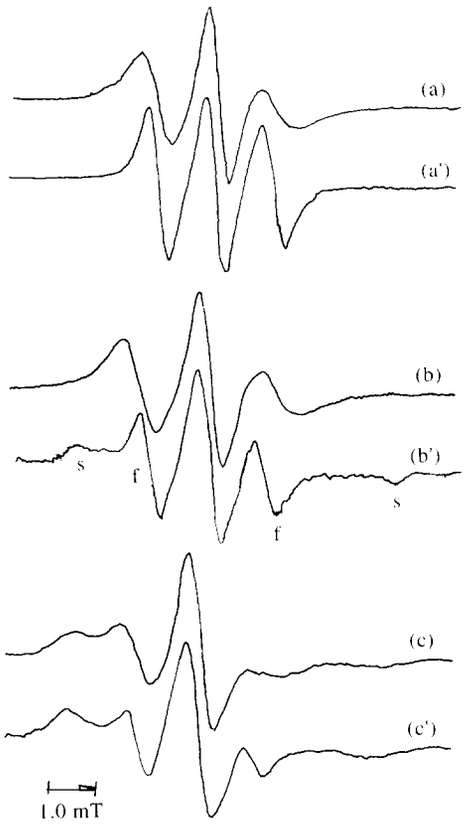

Figure 1 E.s.r. spectra of spin-labelled PS (SL–PS) in solutions of C_6H_{12} (a) and CCl_4 (a') (PS concentration, C_p = 1.5 g/100 ml) and e.s.r. spectra of SL–PS adsorbed on the silicas from the solutions: MB-300 from C_6H_{12} (b) and CCl_4 (b'); MB-800 from C_6H_{12} (c) and CCl_4 (c') (E.s.r. spectra of the residue were observed after the supernatant was removed). Measurements were carried out at room temperature

RESULTS AND DISCUSSION

Adsorption and molecular motion in solutions

Figure 1 shows the e.s.r. spectra of the spin-labelled PS. Spectra (a) and (a') were observed in solutions of C_6H_{12} and CCl_4, whereas spectra (b), (b') and (c), (c') were observed after the PS molecules were adsorbed on the silica surface from the solutions and the solvents in the mixed sample (PS-190/silica gel/solvent) were removed. In general, the spacing between the outermost components of a triplet are caused by the hyperfine interaction with nitrogen nucleus narrowing with an increasing mobility of the radicals because of motional averaging of the anisotropy of the interaction. The complete averaging gives rise to the isotropic and narrowed spectrum. The outermost splitting ($2A_z'$) is a good measure of the mobility of the spin-labelled PS (SL–PS). The isotropic and narrowed spectra are observed in the solutions (*Figure 1a, a'*). The e.s.r. spectrum of the SL–PS in the CCl_4 solution is much narrower than that in the C_6H_{12} solution. The difference in the solvent viscosity of CCl_4 and C_6H_{12} at room temperature is quite small. The solvent viscosity of CCl_4 and C_6H_{12} at 20°C are 0.97 and 0.979 mP s, respectively[14]. The difference is smaller than 0.009 which corresponds to the variation of the viscosity of solvents with an increase of only 0.6°C. Then, it can be considered that the higher mobility of PS in the good solvent of CCl_4 should reflect its larger excluded volume effect. For instance, the solvent molecules are good plasticizers for the expanded conformation of PS.

Only one component, the motionally narrowed spectrum, was also observed in the sample of the PS adsorbed on the MB-300 silica from the C_6H_{12} solution (*Figure 1b*). On the other hand, a two component spectrum with different rates of motion, a 'fast' and a 'slow' component arising from the radicals[15,16], is observed in the samples of the PS on the MB-300 silica from the CCl_4 solution (*Figure 1b'*).

Two component spectra are also observed in the samples of the PS in the MB-800 silica from the C_6H_{12} solution (*Figure 1c, c'*). The nitroxide radicals are affected by their environments, and the fast and slow components spectra (the isotropic and anisotropic spectra) are attributed to the SL–PS weakly and strongly adsorbed on the silica surfaces, respectively. The segments of the strongly adsorbed PS are interacted with the silica by hydrogen bonding. For instance, benzene rings in the PS are bonded to silanol groups in the silica surface. It is found that a part of PS chains in the solution is weakly adsorbed on the silica surface of the MB-300 in C_6H_{12}, whereas more segments are adsorbed by a strong interaction for the MB-300 in the CCl_4 solution and the MB-800 in the C_6H_{12} and CCl_4 solutions. In spite of the higher mobility of the SL–PS in the CCl_4 solution, the slow component spectrum is more remarkable in the samples of the PS adsorbed on the silica from the CCl_4 solution than that from the C_6H_{12} solution. This reflects that more PS segments strongly interacted with the silica in the CCl_4 solution.

Interaction of adsorbed PS with silica gel in dried samples

E.s.r. spectra of SL–PS adsorbed on silica at −196°C. *Figure 2* shows e.s.r. spectra of SL–PS observed at −196°C after the solvent is completely evacuated. The values of the widths between the outermost peaks ($2A'_z$) in the samples of PS in the MB-800 silica (*Figure 2b, b'*) are larger than those in the samples of PS in the MB-300 silica (*Figure 2a, a'*). The values of $2A'_z$ in the samples of PS adsorbed from the CCl_4 solution (*Figure 2a', b'*) than those from the C_6H_{12} solution (*Figure 2a, b*). It can be considered that different values of $2A'_z$ are caused by the effect of PS–silica interaction on hyperfine splitting (h.f.s.) due to nitrogen nucleus. Griffith *et al.*[17,18] showed that there is a small solvent effect on the e.s.r. spectra of nitroxide spin labels and developed a semi-quantitative treatment of this effect. The variations of A_z and g values observed in our study should arise from the electric field of the polar group as concluded by Griffith *et al.* The solvent dependence of e.s.r. spectra can be visualized as arising from changes in the relative contributions of the two valence structures, *A* and *B* of the neutral free radicals.

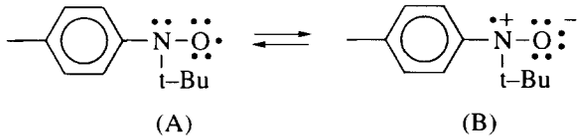

(A) (B)

The changes are caused by the electric field of the silica gel surface. Structure A localizes the unpaired electron on the oxygen atom, whereas structure B localizes it on the nitrogen atom, and the electric field that tends to stabilize B is responsible for the increased splitting due to the nitrogen nucleus and the decreasing g value.

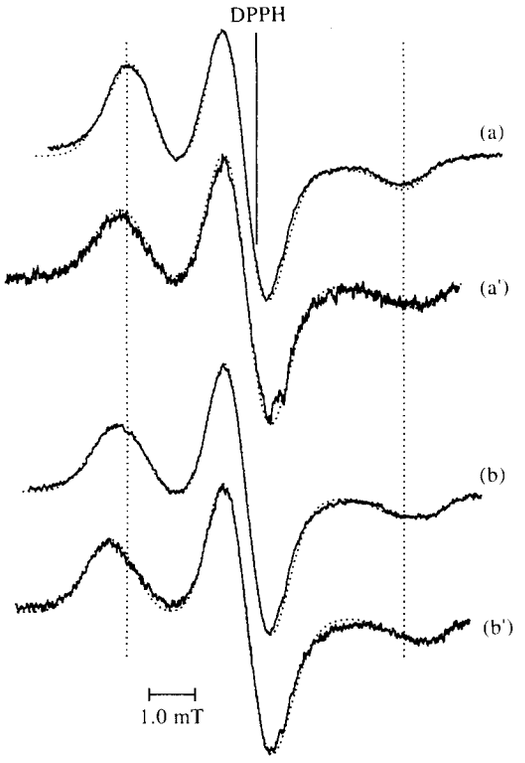

Figure 2 E.s.r. spectra of spin-labelled PS adsorbed on the silicas MB-300 from C_6H_{12} (a) and CCl_4 (a'); MB-800 from C_6H_{12} (b) and CCl_4 (b'). Measurements were carried out at −196°C after the solvents were completely evacuated. Solid and dotted lines are experimental and calculated spectra, respectively

E.s.r. spectrum calculated by assuming two components from two different conformations. In order to obtain the exact e.s.r. parameters, spectral simulations for the e.s.r. spectra are performed. It is found that all spectra for the adsorbed PS are composed of two components, whereas the e.s.r. spectrum for SL–PS in the homopolymer PS (PS bulk) can be simulated by assuming only one component as shown in *Figure 3a*. The spectra for the adsorbed PS are not well resolved and the two components analysis seems meaningless. However, the experimental spectra can never be simulated by only one component. Fortunately, the outermost peak in the high magnetic field is like the plateau in the e.s.r. spectrum of SL–PS adsorbed on the MB-800 silica from the C_6H_{12} solution as shown in *Figure 3b*. The flat peak suggests that the two component analysis is reasonable for the e.s.r. spectrum. The agreement between the simulated spectrum (the dotted line) and the observed spectrum (the solid line) is excellent and indicates the classification of the spin-labels into two kinds of labels (A- and B-labels) affected by different environments is a good approximation. E.s.r. parameters determined from the spectral simulation are indicated in *Table 1*. The high values of A_z (3.62 mT) and $A_i = (A_x + A_y + A_z)/3$ (1.59 mT) for the A-labels are caused by the electric field of the silica surface. For instance, the segments connected with the A-labels are strongly interacted with the silica as 'train' segments.

On the other hand, the values of A_z (2.70 mT) and A_i (1.25 mT) for B-labels are lower than those of SL–PS in

Table 1 E.s.r. parameters of spectra of spin labelled PS, determined from the spectrum simulation mentioned in the text. The values in brackets shown under sample code name mean the size ratio of pore diameter (d) to twice radius of gyration ($2\langle R^2\rangle^{1/2}$)

		MB-300/C_6H_{12} (1.2)		MB-800/C_6H_{12} (3.4)		MB-300/CCl_4 (0.9)		MB-800/CCl_4 (2.5)	
	PS-bulk	A	B	A	B	A	B	A	B
g_z	2.0024	2.0031	2.0029	2.0023	2.0027	2.0026	2.0027	2.0022	2.0027
g_y	2.0072	2.0069	2.0077	2.0063	2.0074	2.0061	2.0072	2.0063	2.0074
g_x	2.0072	2.0069	2.0077	2.0066	2.0079	2.0063	2.0077	2.0067	2.0079
$(g_x+g_y+g_z)/3$	2.0056	2.0056	2.0061	2.0051	2.0060	2.0050	2.0059	2.0051	2.0060
A_z, mT	2.94	3.20	2.66	3.63	2.88	3.62	2.90	3.65	3.02
A_y, mT	0.52	0.49	0.58	0.57	0.56	0.57	0.53	0.62	0.56
A_x, mT	0.52	0.49	0.58	0.57	0.56	0.57	0.53	0.62	0.56
$(A_x+A_y+A_z)/3$	1.32	1.39	1.27	1.59	1.33	1.59	1.32	1.63	1.38
Line width, mT	0.97	0.86	1.08	0.86	0.95	0.86	0.99	0.93	1.40
Fraction (%)	100	50	50	45	55	40	60	76	24

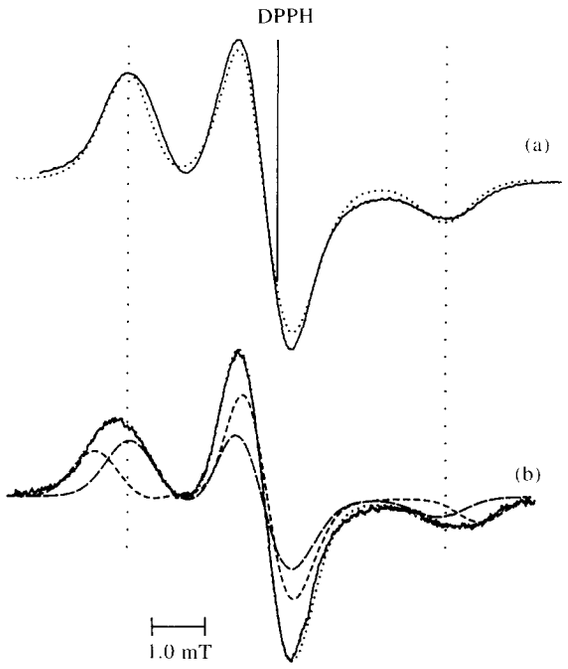

Figure 3 Comparisons of calculated spectra (dotted) and observed spectra (solid) of spin labelled PS. (a) Spin labelled PS in homopolymer PS matrices; spectrum is calculated by assuming only one component. (b) Spin labelled PS adsorbed on the MB-800 silica from C_6H_{12} solution; spectrum is calculated by assuming that the spectrum is composed of two spectra from two different magnitudes of interaction with the silica

the homopolymer PS (PS-bulk). This is a reflection of weak interaction of the B-labels with the silica. The segments connected with the B-labels behave like 'loop' or 'tail' segments on the silica surface. The low value of A_z (2.70 mT) and the high values of A_x and A_y (0.59 mT) are also caused by the motional averaging of the anisotropic h.f.s. interaction. This suggests that some PS segments on the silica surface have already begun to move at −196°C.

Dependence of PS–silica interaction on size ratio of pore diameter (silica) to the radius of gyration (PS). All e.s.r. spectra of SL–PS adsorbed on the silica surface are excellently simulated by the method mentioned above (dotted lines in *Figure 2*). The e.s.r. parameters determined for the spectral simulations are shown in *Table 1*. The following results are found from the simulation.

(a) E.s.r. spectra are composed of two components, a spectrum with a low g_i-value [$g_i=(g_x+g_y+g_z)/3$] and a high A_i value, reflecting a strong PS–silica interaction (A-labels) and another spectrum with a high g_i-value and a low A_i value, reflecting a weak PS–silica interaction (B-labels).
(b) The isotropic hfs value, A_i for the adsorbed PS from the CCl_4 solution is larger than from the C_6H_{12} solution. The value, A_i for the adsorbed PS on the silica with the larger pore diameter is also larger.
(c) The fractional amount of A-labels is larger for the SL–PS adsorbed on the MB-800 silica than that on the MB-300 silica.

The radius of gyration ($\langle R^2\rangle^{1/2}$) of the PS-190 sample in the C_6H_{12} solution can be calculated to be 24.0 nm at 35°C from the relationship between the radius of gyration and the molecular weight[19]. The size ratio of the pore diameter to twice the radius of gyration, ($2\langle R^2\rangle^{1/2}$) is 1.2 for the MB-300 silica. Then, only one PS molecule can be trapped in a pore of the silica. It can be considered that the segmental density is extremely low in the structure of only one PS molecule adsorbed on the pore as schematically shown in *Figure 4a*. The e.s.r. spectrum of the adsorbed spin-labelled PS from the CCl_4 solution is anisotropic and broad in comparison with that from the C_6H_{12} solution (*Figure 1*) as mentioned in the previous section. C_6H_{12} is a Θ solvent and CCl_4 is a good solvent for polystyrene at 35°C, at which the PS molecules are adsorbed in the solutions. The radius of gyration of PS in CCl_4 is about 1.4 times larger than that in C_6H_{12}[11]. Then, the size ratio of the pore diameter to $2\langle R^2\rangle^{1/2}$ value can be estimated to be approximately 0.9. This means that the $2\langle R^2\rangle^{1/2}$ value is larger than the average pore size in the MB-300 silica. Thus, the effective adsorption area for PS-190 molecules should be reduced and the PS molecules have to be distorted to become accessible to the pore inside the MB-300 silica. The distorted segments penetrated into the pore can be pressed by the CCl_4 molecules and then, the adsorbed PS segments from the CCl_4 solution is strongly interacted with the silica interface and molecular mobility is low as shown in *Figure 4a'*. On the other

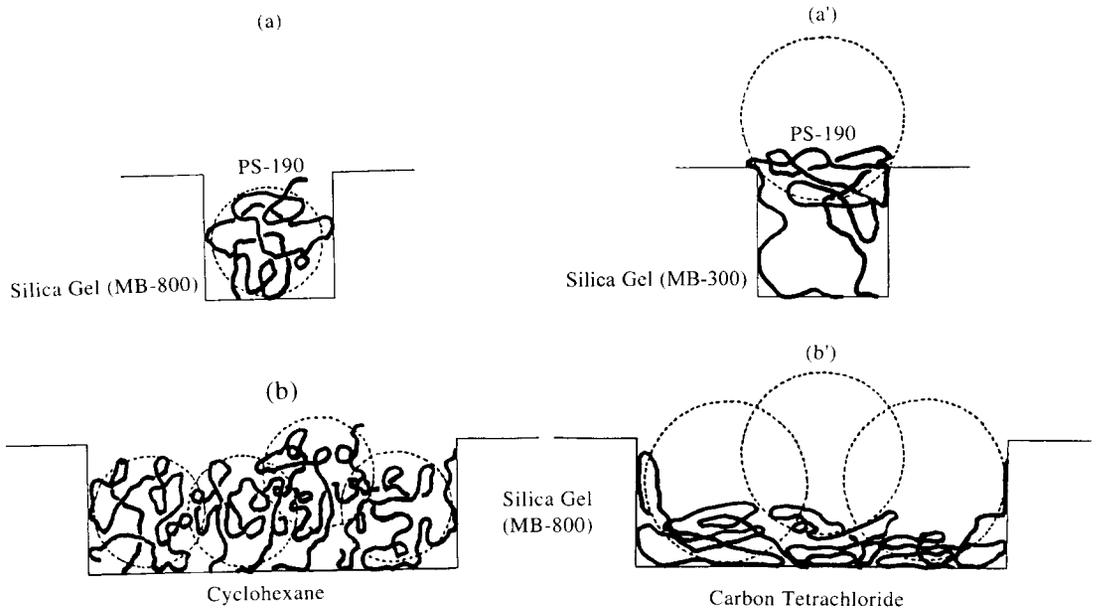

Figure 4 Schematic illustrations of the PS chains adsorbed on the silica surfaces from the solutions. MB-300 from C_6H_{12} (a) and CCl_4 (a'); MB-800 from C_6H_{12} (b) and CCl_4 (b')

hand, several molecules can be penetrated into a pore of the MB-800 silica with a large pore diameter, 81.3 nm, and many segments can be adsorbed on the silica as shown in *Figure 4b*, *b'*. It can be considered that the PS segments are expanded in the larger pore and the segment should be strongly interacted with the silica (*Figure 4b'*). The solvency of C_6H_{12} and CCl_4 affects the intermolecular interaction as well as the intramolecular segment–segment interaction. However, the former interaction seems not to take an important role for the adsorption behaviour.

From these considerations, it is confirmed that the PS segment–silica interaction in the samples prepared from the CCl_4 solution is stronger than that from the C_6H_{12} solution. It is also found that the segments of the adsorbed PS on the silica surfaces with larger pore diameter, MB-800, are more strongly interacted with the silica molecules. From the values of A_z and g values given in *Table 1*, it is concluded that the magnitude of the PS segment–silica interaction has a distribution and the magnitude is a function of the size ratio of the pore diameter, d, to twice the radius of gyration, $2\langle R^2\rangle^{1/2}$ and also affected by the conformation of the PS chains in the Θ and good solvents. The present conclusion is compatible with the results of the adsorption isotherms studied by Kawaguchi *et al.*[10–12]. The plateau adsorbed amount and the kinetic behaviour of the adsorption should be related to the PS–silica interaction. They interpreted the dependencies of solvent and the size ratio of d to $2\langle R^2\rangle^{1/2}$ in terms of a fractal surface with the fractal dimension.

In the dried samples, the evaporation process involves complex and time dependent events, such as precipitation and release of the trapped solvent. However, the results obtained in the present paper indicate that the PS–silica interaction and the conformation of PS in the solution are preserved in the dried samples.

Molecular motion of polystyrene adsorbed on solid surface of silica gel

In order to evaluate the molecular mobility of adsorbed PS chains related to the PS segment–silica interaction, e.s.r. spectra were observed at various temperatures after the solvents were completely evacuated. *Figure 5* shows the temperature dependence of the e.s.r. spectra of the spin-labelled PS on the MB-300 silica from the C_6H_{12} solution. The outermost splitting ($2A_z'$) for the PS adsorbed on the silica from the C_6H_{12} solution are plotted against observation temperature in *Figure 6*. The value of $2A_z'$ is a good measure of the mobility of the spin-labelled PS as mentioned above.

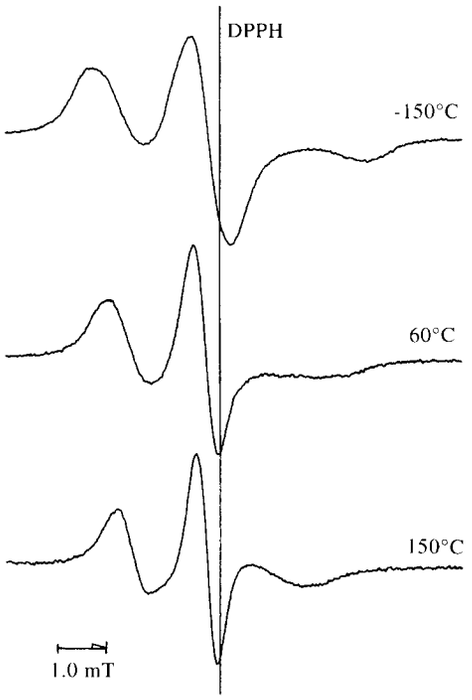

Figure 5 E.s.r. spectra of spin-labelled PS adsorbed on the solid silica surface (MB-300) from the C_6H_{12} solution at various temperatures. Measurements were carried out after the solvents were completely evacuated

PS adsorbed from C_6H_{12} solution and dried. The width narrowed with increasing temperature because of

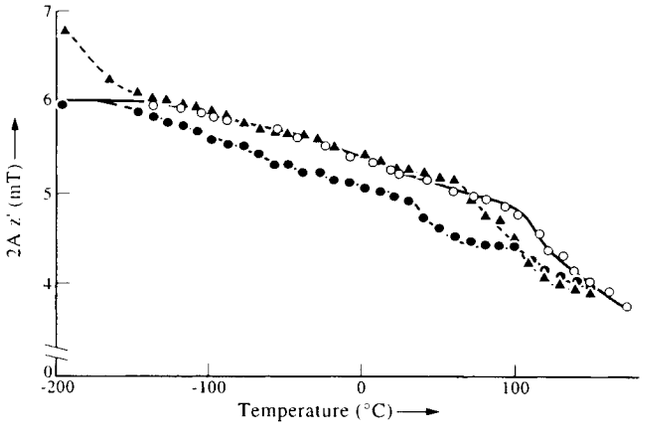

Figure 6 Variation of outermost splitting ($2A_z'$) with temperatures: solid bulk of PS (○); adsorbed PS on the solid silicas, MB-300 (●) and MB-800 (▲) from the C_6H_{12} solution

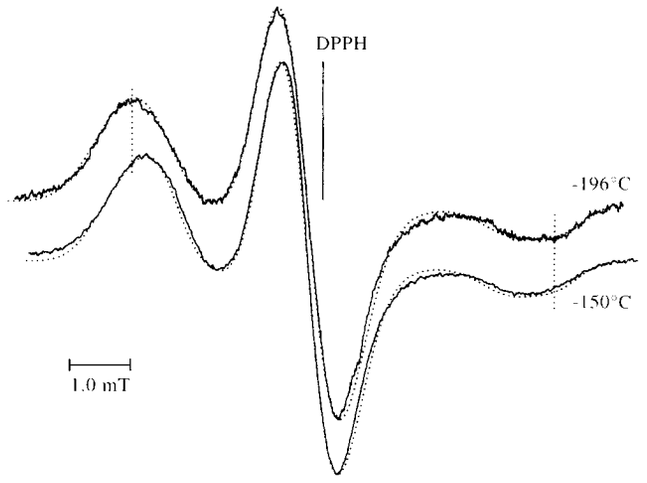

Figure 7 E.s.r. spectra of spin-labelled PS adsorbed on the solid silica surface (MB-800) from the C_6H_{12} solution at −196°C and −150°C. Measurements were carried out after the solvents were completely evacuated. Dotted and solid lines indicate calculated and observed spectra, respectively

increasing averaging of the anisotropy of the hyperfine coupling. In the solid bulk of polystyrene [*Figure 6* (○)], the outermost peaks gradually changed around 60°C and narrowed sharply at 100°C. Decreases of the outermost separation width in the lower and higher temperature ranges are attributed to a local mode relaxation, and a micro-Brownian type molecular motion, respectively[20,21]. On the other hand, in the PS chains adsorbed on the MB-300 porous silica from the C_6H_{12} solution [*Figure 6* (●)], the narrowing curves show remarkable drops in three temperature ranges, near −150 to −20°C, 25 to 50°C and 100 to 150°C. The narrowing curve shifted to lower temperatures than that in the solid bulk of PS. Especially, the rigid-to-isotropic pattern change of the PS sample in the medium temperature range occurred at a temperature 70°C lower than that of the bulk PS. This result indicates an increase in the segmental mobility of only one PS chain in a pore because of the weak interaction of the segment with the silica, reflecting the low segmental density and the excess free volume in comparison with that in the bulk PS. The mobile segments correspond to those connected with B-labels which have low values of A_z and A_i as shown in *Table 1*. The extremely low value of A_z is reflecting the low segmental density. Recently, we studied molecular motion of the radical of polyethylene molecules anchored on a fresh surface of polytetrafluoroethylene, and found the chain end radical allows free rotation around the C–C bond axis even at 196°C. The high mobility is attributed to weak intermolecular forces in the low segmental density[22–24]. The drop in the highest temperature region should be caused by the molecular motion of the segments connected with A-labels which have high values of A_z and A_i as shown in *Table 1*.

The value of $2A_z$ for the spin-labelled PS in the MB-800 silica from the C_6H_{12} solution decreases sharply at −196 to −150°C [*Figure 6* (▲)]. This reversible change (spectral change from the spectrum observed at −196°C to that at −150°C) indicates that a part of the 'train' segments of flatter conformation converts to a 'loop' or 'tail' segment of loopy conformation. *Figure 7* shows e.s.r. spectra of the SL-PS in the MB-800 observed at −150°C in comparison with that observed at −196°C. E.s.r. parameters determined by the simulation mentioned above are also shown in *Table 2*. The fractional amount of A-labels decreases with increasing

Table 2 Temperature dependent e.s.r. parameters of spectra of SL–PS adsorbed on the MB-800 silica

	MB-800/C_6H_{12} −150°C		MB-800/C_6H_{12} −196°C	
	A	B	A	B
g_z	2.0023	2.0025	2.0023	2.0027
g_y	2.0063	2.0072	2.0063	2.0074
g_x	2.0066	2.0078	2.0066	2.0079
$(g_x+g_y+g_z)/3$	2.0051	2.0058	2.0051	2.0060
A_z, mT	3.56	2.82	3.63	2.88
A_y, mT	0.55	0.57	0.57	0.56
A_x, mT	0.55	0.57	0.57	0.56
$(A_x+A_y+A_z)/3$	1.55	1.32	1.59	1.33
Line width, mT	0.74	0.88	0.86	0.95
Fraction (%)	38	62	45	55

temperature. The extreme separation width drastically decreases at *ca.* 50°C lower than that of the bulk PS as shown in *Figure 6*. This transition is a reflection of the conversion of 'train' segments to 'loop' or 'tail' segments. The adsorbed segments begin to protrude from the silica surface when the segments have thermal energy equal to the PS–silica interaction energy. After the release of the interaction, the molecular mobility depends on the segmental density. Because only approximately four PS molecules are adsorbed in a pore of silica gel as shown in *Figure 4b*, the segmental density is much lower than in the bulk PS. Consequently, the molecular motion of the adsorbed PS resulted in being very high.

PS adsorbed from CCl_4 solution and dried. *Figure 8* shows the temperature dependence of $2A_z'$ for the adsorbed PS on the silica from the CCl_4 solution in comparison with that of the bulk PS. In the PS chains adsorbed on the MB-300 silica from the CCl_4 solution, the absolute values of $2A_z'$ are higher and lower than in the solid bulk of PS in the lower and higher temperature ranges, respectively. These experimental facts indicate that the strong PS segment–silica interaction causes a hindrance of the molecular mobility in the lower temperature range, the strong interaction is gradually released and a high molecular mobility can be attained

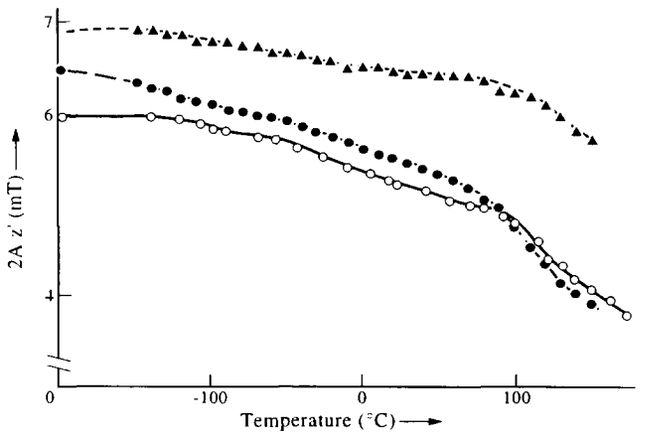

Figure 8 Variation of outermost splitting ($2A_z'$) with temperature: solid bulk of PS (○); adsorbed PS on the silica, MB-300 (●) and MB-800 (▲) from the CCl_4 solution

in the higher temperature range because of the low segmental density. It is very interesting that the conformations of PS chains in the solutions of the Θ and good solvents affect the structures of the weakly and strongly interacting polymer–solid surface and the molecular mobility of the polymer chains in the dried samples. It was also found that the $2A_z'$ vs temperature curve for the adsorbed PS on the MB-800 silica shifted to higher temperatures. Surprisingly, the variation in the lower temperature range is very small for the PS adsorbed from the CCl_4 solution. This fact suggests that the very strong PS segment–silica interaction causes a hindrance to the mobility associated with the local mode relaxation. Almost all segments have a flatter conformation as 'train' segment in a pore of the MB-800 silica, whereas the more segments have a more loopy structure in a pore of the MB-300 silica. It can be considered that the magnitude of the molecular mobility of the adsorbed PS is a decreasing function of the segment–silica interaction and the segmental density.

We will study the structure of the polymer chains with different molecular weights at the porous silica surfaces and publish in a forthcoming paper.

REFERENCES

1 Takahashi, A. and Kawaguchi, M. *Adv. Polym. Sci.* 1982, **46**, 1
2 Alster, J. V. and Ovenall, D. M. *Polym. Commun.* 1991, **32**, 549
3 Chakraborty, A. K. and Adriani, P. M. *Macromolecules* 1992, **25**, 2470
4 Gambogi, J. E. and Bulum, F. D. *Macromolecules* 1992, **25**, 4526
5 Ei-Hakim, A. A. A., Ramadan, A. M. and Badran, A. S. *Polymer* 1992, **33**, 4880
6 Kobayashi, K., Araki, K. and Imamura, Y. *Bull. Chem. Soc. Jpn.* 1989, **62**, 3421
7 Kobayashi, K., Yajima, H., Imamura, Y. and Endo, R. *Bull. Chem. Soc. Jpn.* 1990, **63**, 1813
8 Kawaguchi, M., Maeda, K., Kato, T. and Takahashi, A. *Macromolecules* 1984, **17**, 1666
9 Thambo, G. and Miller, W. G. *Macromolecules* 1990, **23**, 4397
10 Kawaguchi, M. and Arai, T. *Macromolecules* 1991, **24**, 889
11 Kawaguchi, M., Anada, S., Nishikawa, K. and Kurata, N. *Macromolecules* 1992, **25**, 1588
12 Anada, S. and Kawaguchi, M. *Macromolecules* 1992, **25**, 6824
13 Bullock, A. T., Cameron, G. G. and Smith, P. M. *J. Phys. Chem.* 1973, **77**, 1635
14 Kagaku Binrun II, *The Chem. Soc. Jpn*, Maruzen, Tokyo, 1993
15 Cameron, G. G., Miles, I. S. and Bullock, A. T. *Br. Polym. J.* 1987, **19**, 129
16 Shimada, S., Kashima, K., Hori, Y. and Kashiwabara, K. *Macromolecules* 1990, **23**, 3769
17 Griffith, O. H., Dehlinger, P. J. and Van, S. P. *J. Membr. Biol.* 1974, **15**, 159
18 Shimada, S., Hori, Y. and Kashiwabara, K. *Macromolecules* 1988, **21**, 3454
19 Beery, G. C. *J. Chem. Phys.* 1966, **44**, 4550; 1967, **46**, 1338
20 Tsay, F. and Gupta, A. *J. Polym. Sci. Polym. Phys. Ed.* 1987, **25**, 855
21 Shimada, S. *Prog. Polym. Sci.* 1992, **17**, 1
22 Sakaguchi, M., Yamaguchi, T., Shimada, S. and Hori, Y. *Macromolecules* 1993, **26**, 2612
23 Sakaguchi, M., Shimada, S., Hori, Y., Suzuki, A., Kawaizumi, F., Sakai, M. and Bandow, S. *Macromolecules* 1993, **26**, 2612
24 Shimada, S., Suzuki, A., Sakaguchi, M. and Hori, Y. *Macromolecules* 1993, **26**, 2612